# A three dimensional model of primary bovine endometrium using an electrospun scaffold

MacKintosh, S.B.[1,2], Serino, L.P.[3], Iddon, P.D.[3], Brown, R.[4], Conlan, R.S.[1], Wright, C.J.[4], Maffeis, T.G.G.[4], Raxworthy, M.J.[3], Sheldon, I.M.[1].

*[1]Institute of Life Science, College of Medicine, Swansea University, Singleton Park, Swansea, SA2 8PP, United Kingdom. [2]Department of Veterinary Clinical Sciences, Royal Veterinary College, Royal College Street, London, NW1 0TU, United Kingdom. [3]Neotherix Ltd., Research Centre, York Science Park, York, YO10 5DF, United Kingdom. [4]College of Engineering, Swansea University, Singleton Park, Swansea, SA2 8PP, United Kingdom.*

**Corresponding author:**

Siân MacKintosh*, Institute of Life Science, School of Medicine, Swansea University, Singleton Park, Swansea, SA2 8PP, United Kingdom. sim17@aber.ac.uk.

* S. MacKintosh present address: IBERS, Gogerddan, Aberystwyth University, Aberystwyth, Ceredigion, UK, SY23 3EE.

**Abstract**

Endometrial stromal and epithelial cell function is typically studied *in vitro* using standard two dimensional (2D) monocultures, but these cultures fail to reflect the complex 3D architecture of tissue. A 3D model of bovine endometrium that reflects the architectural arrangement of *in vivo* tissue would beneficially assist the study of tissue function. An electrospun polyglycolide (PGA) scaffold was selected to grow a 3D model of primary bovine endometrial epithelial and stromal cells, that reflects the architecture of the endometrium for the study of pathophysiology. Electrospun scaffolds were seeded with stromal and epithelial cells, and growth was assessed using histological techniques. Prostaglandin $E_2$ and prostaglandin $F_{2\alpha}$ responsiveness of endometrial scaffold constructs was tested using oxytocin plus arachidonic acid or lipopolysaccharide (LPS). Stromal and epithelial cells growing on the electrospun scaffold had an architectural arrangement that mimicked whole tissue, deposited fibronectin, had appropriate expression of vimentin and cytokeratin and were responsive to oxytocin plus arachidonic acid and LPS, as measured by prostaglandin accumulation. In conclusion, a functional 3D model of stromal and epithelial cells was developed using a PGA electrospun scaffold which may be used to study endometrial pathophysiology.

**Key words:** Scaffold; polyglycolide; SEM; in vitro test; co-culture; uterus

## 1. Introduction

Recent advances in tissue engineering have facilitated the development of 3D tissue constructs using a scaffold based approach, where the scaffold serves to mimic the extracellular matrix (ECM) of tissue to provide a framework for cell growth [1, 2]. Typically, tissue engineering aims to produce tissue constructs for implantation in the event of injury, such examples include skin, cartilage and bone [3-5]. The development of a bioartificial uterus for uterine transplantation and, potentially, ectogenesis has also been considered [6]. However tissue engineering may also provide test-bed material for *in vitro* research, which may assist the development of therapies for disease [7]. The development of a defined three dimensional (3D) endometrial tissue construct would be advantageous for the *in vitro* study of endometrial function. Whilst 2D monoculture of cells on flat culture plates has hugely advanced our understanding of cell function, and will continue to do so, 2D monocultures do not reflect the heterogeneous cell population and 3D architecture of tissue; and these features would be better represented by a 3D model [8, 9].

The endometrium, which consists of a polarised, columnar epithelium overlaying stromal cells and also immune and endothelial cells, is an endocrine mucosal tissue. In cattle, the endometrium has key roles in reproduction, including regulation of the reproductive cycle, providing a site for implantation and acts a barrier between the uterine lumen and the deeper tissues of the uterus. Development of a 3D endometrial construct would facilitate not only the study of endometrial cell, but also tissue function. Development of 3D models of human endometrium are emerging, and the use of these models to study features such as implantation or steroid responsiveness demonstrates the potential of tissue engineered constructs for the study of endometrial function [10, 11]. Species-specific models are of key importance due to major species-specific differences in tissue function, but also variation in the culture procedures of endometrial cells from different species. For bovine endometrium, a heterocellular spheroid model of bovine endometrial stromal and epithelial cells was achieved by culturing cells in ascorbate [12], but this model may offer little control over the shape of the model formed. The aforementioned human endometrial models utilised

scaffolds formed from biological polymers, which are associated with high bio-compatibility [13]. In contrast, synthetic polymers are suited for the development of large scale, high throughput experimentation that can be adapted for scaffold design, strength and bio-degradability, but may be less biocompatible [6, 13].

Polyglycolide (PGA) is a synthetic polymer which has previously been used to support the growth of a wide variety of cell types including, fibroblasts and epithelial cells for the repair of abdominal wall tissue, urethral tissue and intestine [14-16]. The PGA polymer has good potential for high biocompatibility with reproductive tissues, as it is a recommended suture material for perineal repair, but is also associated with minimal inflammatory reactions when used as a suture material for oral tissues compared to silk sutures [17, 18]. Ideally, a biodegradable scaffold degrades at the same rate of cellular division and ECM deposition, maintaining structure integrity and resulting in a construct that is predominantly of native ECM and cells [19].

In addition to polymer selection, scaffold design is also important. The scaffold should have a high surface area to volume ratio, high reproducibility, stimulate ECM deposition, and suitable porosity that enables cellular infiltration, three dimensional growth and diffusion of nutrients and waste products [2, 20, 21].

The electrospun model is a well characterised scaffold design that addresses many of the key requirements for tissue engineering. The electrospun scaffold provides a dense mesh, mimicking the complex architecture of native tissue, with high porosity that may be altered during production [22-24]. An electrospun PGA scaffold has been previously used to grow skin constructs, supporting human dermal fibroblasts [25], and may provide a suitable scaffold for supporting endometrial cell growth.

The present study aimed to generate a functional reconstitution of bovine endometrium using epithelial and stromal cells on a synthetic polymer scaffold. The objectives were to i.) establish a stromal cell population onto the PGA electrospun scaffold, ii.) develop a co-culture construct of epithelial and

stromal cells, iii.) evaluate the co-culture construct and iv.) test the functional response of the endometrial construct. Functionality of the endometrial constructs were tested by measuring the accumulation of prostaglandin $E_2$ (PGE) and $F_{2\alpha}$ (PGF) following treatment of constructs with oxytocin plus arachidonic acid (OT+AA), or *Escherichia coli* lipopolysaccharide (LPS), as patho-physiological model of bovine endometritis, as achieved previously using 2D monocultures [26, 27].

## 2. Materials and Methods

### *2.1 Preparation of Electrospun Scaffold*

1,1,1,3,3,3-Hexafluoro-2-propanol (HFIP) 99.9% was purchased from Apollo Scientific Ltd and used without further purification. PGA was purchased from PURAC Biomaterials and used after melt-extrusion and subsequent quenching in water to obtain a HFIP-soluble polymer. The final weight-average molecular weight of the vacuum-dried extruded PGA was approximately 100,000. The molecular weight of the PGA was measured by size exclusion/gel permeation chromatography (GPC). Briefly, a portion of each sample was taken and dissolved in HFIP, to give solutions with a concentration of around 0.2%. The HFIP contained 0.5 µL/mL of benzyl alcohol to be used as a flow rate marker. Samples were left overnight before being filtered through 0.45 µm PTFE filters prior to analysis. All sample solutions were run in duplicate, and calibration was carried out using poly(methyl methacrylate) Easivial calibrants (Polymer Laboratories). The following GPC conditions were used: two PL HFIP-gel 300 x 7.5mm columns; HFIP eluent at 1.0 mL/min; 50 µL injection; and refractive index detection at 40 ℃

The extruded PGA was used to prepare 11.5 w/w % solutions of PGA in HFIP, which were rolled overnight to allow complete dissolution. Prior to electrospinning, the solutions of PGA in HFIP were filtered into syringes through 10 µm polypropylene filters. The syringes containing the filtered solutions were loaded into two syringe pumps, set to dispense the polymer solutions at a flow rate of 0.04 mL/min per needle via HFIP-resistant tubing connected to four flat-ended 21 gauge steel needles. The needles were arranged in two pairs, each pair on opposite sides of an earthed 50 mm diameter, 200 mm long steel mandrel (the needles in each pair were aligned perpendicularly with respect to the rotational axis of the mandrel) (Figure 1). The needle tip to mandrel separation distance was set to 150 mm. The mandrel was completely covered in a sheet of non-stick release paper and rotated at 50 rpm. A positive potential difference of 11.0 kV relative to earth was applied to the needles. Electrospun fibres were then formed from the solution delivered to the needle tips, and collected on the paper-covered

mandrel to form a non-woven scaffold sheet. Electrospinning was carried out at 19 ℃ and a relative humidity of approximately 38%. After fibre deposition was complete the scaffold was removed from the mandrel and then dried under vacuum at room temperature for at least 72 hours.

Following drying, the scaffolds were cut into 13 mm discs and stored under air in sealed moisture barrier pouches containing desiccant. These pouches were then sterilised by gamma irradiation.

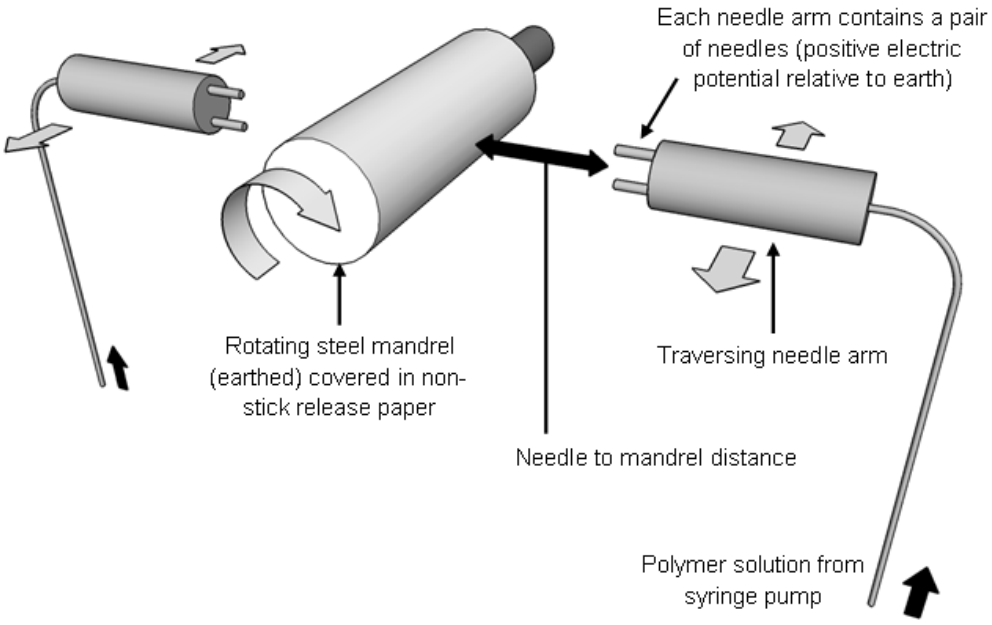


Figure 1. A sketch showing the equipment set-up for electrospinning. A polymer solution is released from two pairs of syringes which were mounted at opposite sides of the mandrel, and aligned perpendicularly with respect to the rotational axis of the mandrel (50 rpm). The needle tip to mandrel separation distance was set to 150 mm. Electrospun fibres were collected on the paper-covered mandrel to form a non-woven scaffold sheet.

The scaffold architecture was characterised by analysis of scanning electron microscopy (SEM) images in order to calculate the mean fibre diameter and by capillary flow porometry in order to determine the pore size distribution. For SEM characterisation, the sample was attached to an SEM stub, sputter coated with gold/palladium alloy and then imaged by an FEI-Quanta Inspect SEM in the high vacuum mode using a voltage of 5.0 kV and spot diameter of

2.5 nm. Three SEM images were processed using GIMP 2.6.6 software in order to calculate the mean fibre diameter. For each image, the diameters of the first 20 clearly visible fibres along a randomly selected straight line were measured; the aggregate 60 measurements were then used to calculate the scaffold mean fibre diameter and standard deviation.

Capillary flow porometry analysis was carried out on 26 mm diameter scaffold discs using a PMI Capillary Flow Porometer CFP-1100-AEXL. The wetting fluid used was Galwick (surface tension 15.9 dyn/cm) and the test method used was Dry Up/Wet Up with a maximum pressure of 5 psi. Of the data generated, the three values *Largest Detected Pore Diameter* (pore diameter at the bubble point), *Mean-Flow Pore Diameter* (median pore diameter), and *Diameter at Maximum Pore Size Distribution* (peak pore diameter) were chosen to best represent the through-pore size distribution of the scaffolds.

### *2.2 Isolation of endometrial cells*

Uteri of the early-luteal phase (days 1-4 of oestrous cycle) were collected from an abattoir from non-pregnant cattle (*Bos taurus*) under 30 months of age, immediately following slaughter, with approval of the Local Ethical Review Panel and the UK Food Standards Agency. Stage of cycle was determined by ovarian morphology, as previously described [28].

Uteri were transported to the laboratory on ice within 2 h, for immediate processing. Endometrial cells were isolated independently from the uteri of a total of 15 animals for the study, with each individual experiment using cells isolated from 3 uteri, unless otherwise stated. The experiments used technical replicates of at least two culture wells for each treatment for each uterus. Dissection and isolation of endometrial cells was performed as previously described [29, 30]. Briefly, the endometrium was dissected from the uterine horn ipsilateral to the corpus luteum. Dissected tissue was incubated in 25 ml digest solution, containing bovine serum albumin (1 mg/ml, BSA; Sigma, Poole, UK), trypsin EDTA (2.5 BAEE units/ml; Sigma), collagenase II (0.5 mg/ml; Sigma) and DNAse I (0.1 mg/ml; Sigma) in Hanks Buffered Saline Solution (HBSS; Sigma) in a shaking water bath for 1 h at 37°C. The digest

solution was filtered through a 40 µm mesh cell strainer, and the filtrate was washed twice by dilution in 10% heat-inactivated foetal bovine serum (FBS, Biosera, East Sussex, UK) in HBSS and centrifugation at 700 × g for 7 min. The resulting cell pellet, containing epithelial and stromal cells, was re-suspended in culture media containing 10% FBS, streptomycin (50 µg/ml; Sigma), and penicillin (50 IU/ml; Sigma) amphotericin B (2.5 µg/ml; Sigma) in RPMI 1640 (Sigma). The heterogeneous cell population was seeded at 1 × $10^5$ cells/ml into 75 $cm^2$ culture flasks (Greiner BioOne, Gloucestershire, UK), and the stromal and epithelial cells were separated by their differential plating times, as described previously [29]. This method results in epithelial and stromal cell populations that are negative for CD45 mRNA [26]. Isolated epithelial and stromal cell purity was >95% as determined microscopically, based upon the morphological differences between the cell types, as reported previously [30]. All cell cultures were incubated at 37℃ in a humidified incubator with 5% $CO_2$ in air, with media changes every 48 h, unless otherwise stated.

Once the cell populations were ~70% confluent, they were transferred from the culture flask to final seeding environment using accutase (Sigma), according to manufacturer's instructions. The resulting cell pellet was re-suspended in culture media for cell seeding, as described subsequently.

### *2.3 Cell culture studies*

*2.3.1 Assessment of cellular attachment and proliferation within the scaffold*

The PGA electrospun discs (13 mm diameter) were mounted in a minusheet (Minucells and Minutissue Vertriebs GmbH, Bad Abbach, Germany), and used in conjunction with 24-well plates. Scaffolds were wetted by immersion in 300 µl culture media for 20 min. Wetting media was discarded before seeding either epithelial or stromal cells (3 × $10^4$ cells/scaffold in 200 µl culture media). Cells were incubated for 4 h before adding a further 800 µl culture media to each well. Monoculture scaffolds were cultured for 7 days before the whole scaffold construct was assessed for cellular attachment using confocal microscopy. Alternatively, PGA scaffolds were seeded with 1 × $10^5$ stromal cells/scaffold alone, or co-cultured with epithelial cells (5 × $10^4$

epithelial cells/scaffold) seeded 24 h after stromal seeding, for analysis of cell viability. Cell viability was measured on days 1, 7 and 10 of culture by MTT. During culture, cell-seeded scaffolds were maintained in a humidified incubator at 37℃ with 5% $CO_2$ in air. Media was changed after 24 h to remove non-adhered cells, and then every 48 h.

*2.3.2 Establish a stromal cell population on the scaffold*

Subsequent 3D cell cultures used PGA electrospun scaffold 13 mm discs secured to the well of a 6-well culture plate (TPP) using an 8 mm cloning ring (Sigma). Scaffolds were pre-wetted with 300 µl culture media applied inside the cloning ring. Stromal cells were seeded onto the wetted scaffold at a density of $1 \times 10^5$ cells/scaffold in 200 µl culture media (day 0 of scaffold culture). After 4 h, a further 100 µl and 3000 µl culture media was applied to the inner and outer compartments of the cloning ring respectively. Scaffolds were maintained as stromal monocultures for 14 days, with media changes every 48 h during the first 10 days of culture, and then every 24 h for the remaining culture period. On days 1, 7, 10, 14 stromal-seeded scaffolds were assessed for histological analysis – using either confocal microscopy, or following paraffin wax-embedding and sectioning for haematoxylin and eosin staining, immunohistochemistry or SEM analysis.

*2.3.3 Develop a co-culture construct of epithelial and stromal cells*

For co-culture endometrial constructs, the stromal cell populated-electrospun PGA scaffolds were seeded with $5 \times 10^4$ epithelial cells/scaffold at i.) 24 h after stromal cell seeding (day 1 of scaffold culture; CCd1) or ii.) on day 7 of scaffold culture (CCd7). Scaffold constructs were cultured up to a maximum of 14 days, with media changes every 48 h until day 10 of culture, and then every 24 h thereafter. Endometrial constructs were removed from culture on days 1, 2, 7, 10 and 14 for histological analysis.

*2.3.4 Test functionality of endometrial constructs*

The physiological and pathological responsiveness of endometrial cells grown on PGA electrospun scaffolds was tested. Co-culture (CCd1) endometrial constructs (n = 18 scaffolds seeded separately with endometrial cells isolated

from 3 uteri) were treated on day 10 of culture with control media, 100 nM oxytocin (Bachem, St Helens, UK) plus 100 µM arachidonic acid (Sigma) or 1 µg/ml O111:B4 ultrapure *Escherichia coli* LPS (Invivogen, Wiltshire, UK) for 24 h. Following cell treatment, the supernatants were collected and stored at -20°C for later analysis by radioimmunoassay (RIA).

### *2.4 MTT*

Changes in the proliferation of viable cells seeded on electrospun scaffolds were evaluated by the 3-(4,5-dimethylthiazol-2-yl)2-5diphenyl-tetrazolium bromide (MTT) assay. Scaffold constructs were transferred to fresh 24-well culture plates for MTT analysis to ensure analysis of only cells growing on the scaffolds. Scaffold constructs were immersed in 500 µl MTT solution (10 mg/ml) in culture media and incubated at 37°C in a humidified incubator with 5% $CO_2$ in air for 2 h. The MTT solution was discarded and 500 µl dimethyl sulfoxide (DMSO, Sigma) was added to lyse cells and dissolve the formazan crystals. The optical density of DMSO-formazan solution (100 µl/well) was measured in a 96-well plate (TPP) using a plate reader (Polarstar Omega; BMG Labware, Aylesbury, UK) at 570 nm absorbance. The MTT results for the electrospun scaffolds are reported as OD.

### *2.5 Fixation of scaffold constructs*

Scaffold constructs were fixed in the culture well following removal of culture media and washing twice with Dulbecco's Phosphate Buffered Saline (DPBS; Sigma) for 5 min. Constructs were immersed in 2% paraformaldehyde (PFA; Sigma) for 5 min, prior to washing three times in DPBS. Scaffold constructs were stored in 0.2% sodium azide in DPSB at 4°C, for later processing.

### *2.6 Wax embedding and sectioning of scaffolds*

Scaffold constructs that had been previously fixed in PFA were processed by hand, by immersion in 70%, 90%, 100%, 100%, 100% industrial methylated spirit (IMS) for 30 min each, 1:1 mixture of 100% IMS:100% xylene for 45 min, 100% xylene overnight, 100% xylene for 30 min, and finally 2 changes of paraffin wax (Taab, Berkshire, UK) for 2 h each.

Following processing, scaffold constructs were embedded in paraffin and cut into 6 µm transverse sections using a microtome (Microtome HM360; Richard Allen Scientific, ThermoFisher, Hertfordhshire, UK) and mounted onto superfrost slides (VWR, Leicestershire, UK). Sections were cut as 10 serial sections, at 30 step intervals.

### *2.7 Immunohistochemistry*

Primary antibodies used for immunohistochemistry (IHC) included rabbit anti-cytokeratin (Abcam, Cambridgeshire, UK), mouse anti-vimentin (Abcam), mouse anti-zona occludens I (Invitrogen, Paisley, UK), mouse anti-fibronectin (Abcam), and Alexa Fluor 555 phallodin (Invitrogen), and were diluted 1:100 in tris-buffered saline (TBS) plus 1% BSA. Secondary antibodies were donkey anti-mouse Alex 488 (Molecular Probes, Invitrogen) and donkey anti-rabbit 555 (Molecular Probes), diluted 1:800 in TBS plus 1% BSA. Immunhistochemistry (IHC) was performed on either intact, PFA fixated, non-paraffin embedded intact scaffold constructs (whole mount scaffolds) or on sections from wax-embedded scaffold constructs. Wax embedded scaffolds were de-waxed in two changes of xylene for 2 min each, and rehydrated through a series of graded alcohol (100%, 90%, 70%, 50%) and distilled water for 2 min each. Rehydrated slides were incubated in a pressure cooker at boiling point with sodium citrate, pH 6.0 for 3 min. Slides were rapidly cooled under a running tap for 10 min. Slides were washed in TBS containing 0.025% Triton X-100 (Sigma), before blocking in 5% donkey serum diluted in 1% BSA in TBS for 2 h. Slides were incubated overnight in primary antibody at 4℃. Following three washes in 1% BSA in TBS for 5 min each, slides were incubated in secondary antibody for 1.5 h at room temperature, in darkness. Slides underwent a final three washes in 1% BSA in TBS, and were mounted using DAPI/Vectashield (H-1200, Vector Labs Inc, Peterborough, UK). Slides were imaged using an upright microscope with fluorescence (Axio Imager M1, Zeiss, Hertfordshire, UK), fitted with a digital camera and processed using Axiovision software (Zeiss).

For whole mount scaffold constructs, the PFA-fixed constructs were washed three times for 5 min each in IHC wash buffer, containing 0.2% sodium azide,

0.2% powdered milk, 2% normal goat serum, 1% BSA, 0.1 M glycine, 0.01% Triton X-100 in phosphate buffered saline (PBS, Sigma). Scaffolds were blocked in 1% donkey serum and 5% BSA in PBS for 1 h, prior to incubation in primary antibody solution at 4°C. Scaffold constructs were washed three times for 5 min each in IHC wash buffer before incubation in secondary antibody for 1 h at room temperature, in darkness. Secondary antibody was removed by three washes in IHC wash buffer for 5 min each, before mounting on glass slide using mounting medium containing 50% glycerol, 25 mg/ml sodium azide and 1 µg/ml Hoechst 33258 (Invitrogen) in PBS. Whole mount scaffold constructs were imaged using a confocal microscope (Zeiss LSM 710, Zeiss) and Zen software (Zeiss), using 10x Plan-Neofluar, 20x Plan Neoflar and 40x C-Apochromat (na = 1.3) objectives with Helium-Neon (543 nm) and Krypton-Argon (405, 488 nm lasers, enabling z-stack imaging of red, green and blue channels.

### *2.8 Haematoxylin and eosin*

Wax embedded sections were stained using haematoxylin and eosin after being de-waxed in three changes in 100% xylene for 5 min each, and rehydrated in 100%, 90%, 70% ethanol and distilled water for 1 min each. Slides were immersed in haematoxylin (Merck, Hertfordshire, UK) for 6 min, before washing in tap water for 5 min and immersion in 0.5% eosin (Merck) for 6 min. The slides were rinsed in tap water, and dehydrated in 70%, 90% and 100% ethanol for 30 sec each. Finally slides were immersed in two changes of 100% ethanol for 2 min each, followed by three changes of 100% xylene for 5 min each. Slides were mounted using dinbutyl phthalate in xylene neutral mounting media (DPX; Taab).

### *2.9 SEM of cell-seeded scaffolds*

Paraffin wax-embedded transverse sections of stromal cell-seeded scaffolds were imaged using SEM to measure the infiltration and growth of cells upon the scaffold. Stromal cells were isolated from three separate uteri and were assessed on day 1, 7 and 10 of culture. Scaffold sections were de-waxed in two changes of 100% xylene for 5 min and allowed to air dry. Slides were imaged without sputter coating, using a field emission scanning electron

microscope (Hitachi S4800) operating at a low accelerating voltage (1 kV). Scaffold constructs were measured for the following: A) the cross sectional depth of the tissue (tissue thickness), measured from the uppermost cell to the deepest cellular material within the scaffold at that measurement point, B) the full cross sectional depth of the entire scaffold construct, including the cellular mass (whole construct thickness), C) the cross sectional depth of the scaffold fibres only, ignoring any cellular material growing on top of the scaffold (Scaffold thickness) (Figure 2). Fifteen measurements were taken for 'B' and 'C' and averaged per uterus, whereas 45 measurements per uterus were taken to assess tissue depth 'A', due to the greater variability in the latter. From these measurements the cellular infiltration was calculated using the following equation:

Cell infiltration = Tissue thickness– (Construct thickness – Scaffold thickness)

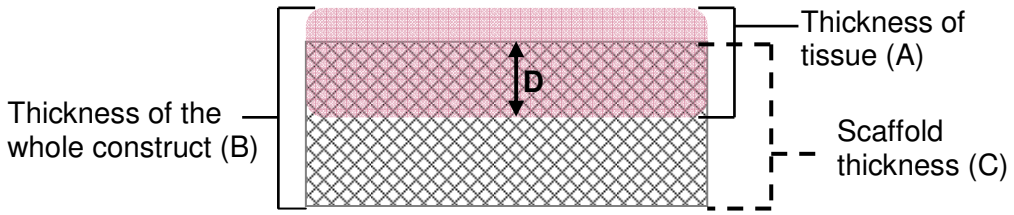


Cell Infiltration into scaffold (D) =
"A" Thickness of tissue – ("B" Whole construct thickness – "C" Scaffold thickness)

**Figure 2. A sketch to depicting the cross sectional measurements taken from 6 µm cross sections of cell-seeded scaffolds.**

### *2.10 Radioimmunoassay*

Cell culture supernatants were analysed for PGE and PGF concentration using radioimmunoassay (RIA) as previously reported [31]. The supernatants, PGE and PGF serum (Sigma) standards, and PGE and PGF tracers (GE Healthcare, Buckinghamshire, UK) were diluted in 0.1% gelatin and 0.01% sodium azide in 0.05 M TRIS buffer as appropriate. Antisera were a generous gift from Prof. N.L. Poyser (University of Edinburgh, Edinburgh, UK). Cross reactivity of antisera were 0.74% and 0.54% for PGE and PGF, respectively [32]. The limits of detection were 2 and 1 pg/tube for PGE and PGF,

respectively [31]. The intra- and inter-assay coefficients of variation were 4.4. and 7.8% for PGE, and 5.1% and 9.7% for PGE, respectively.

### *2.11 Statistics*

Data represent the mean ± SEM and were analysed using PASW statistics (v. 18, SPSS Inc, Hampshire, UK). Data for proliferation on electrospun scaffolds were compared using repeated measures analysis of variance (ANOVA). The effect of treatment with OT+AA or LPS was assessed using ANOVA and Bonferroni post hoc test was used to make pairwise comparisons of $\log_{10}$ transformed data. Significance was assigned where $P < 0.05$.

## 3. Results

*Preliminary assessment of the PGA scaffold*

The electrospun PGA fibres were produced as a 100 µm thick sheet which had a dense mesh-like morphology, as confirmed by SEM (Fig. 3). The electrospun scaffold fibre and porosity characteristics are reported in Table 1.

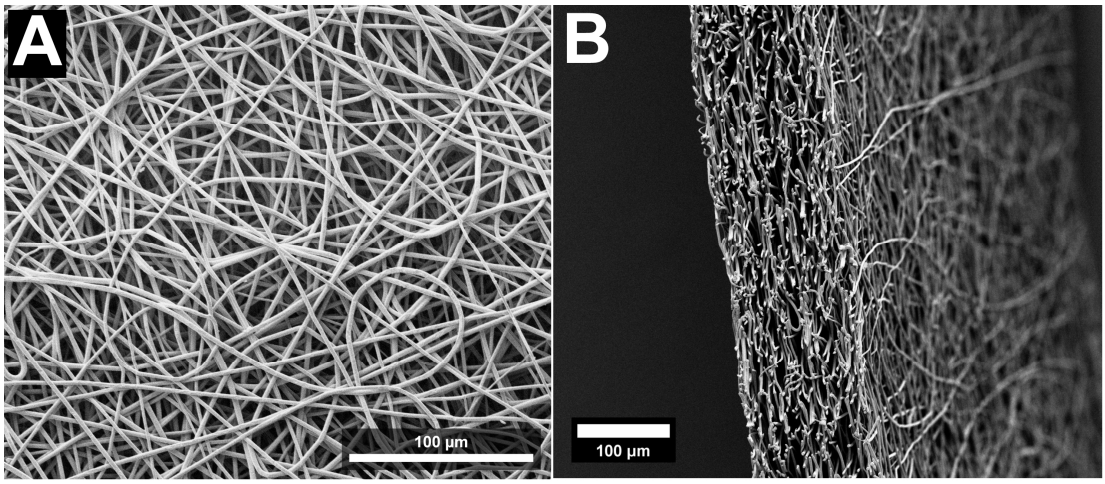


**Figure 3. Scanning electron microscope image of an electrospun PGA scaffold prior to cell seeding.** A) The upper surface of scaffold sheet. B) A cross sectional view of the scaffold. Scale bars = 100 µm.

**Table 1. Electrospun scaffold physical characteristics**. Scaffold thickness was measured along the length of the scaffold sheet using Mitutoyo Absolute Digimatic digital callipers. Mean fibre diameter was measured from 3 SEM images of each scaffold sheet using the first 20 clearly visible fibres/image for each scaffold. The mean-flow pore diameter (median pore diameter), diameter at maximum pore size distribution (peak pore diameter), and pore diameter at the bubble point (largest detected pore diameter) were measured using a PMI Capillary Flow Porometer CFP-1100-AEXL.

| Scaffold thickness (μm) | Mean fibre diameter (μm) | Mean-flow pore diameter (μm) | Peak pore diameter (μm) | Largest pore diameter detected (μm) |
|---|---|---|---|---|
| 100 - 110 | 2.57 ± 0.07 | 7.83 ± 0.11 | 7.45 ± 0.19 | 11.3 ± 0.16 |

Stromal and epithelial cell attachment and growth on the electrospun PGA scaffold was confirmed using IHC and by MTT (Fig. 4). Expression of the cytoskeleton filament, actin, by stromal and epithelial cells grown on electrospun scaffolds for 7 days is shown in Fig. 4(a) and (b) respectively. Distinct differences are apparent in the actin filament structure, with stromal cells exhibiting a strong, filamentous expression, whereas the epithelial actin filaments had strong expression, but were less defined (Fig. 4(a-b)). Interestingly, the scaffold fibres auto-fluoresced (shown in blue), providing a clear view of the actin filament interaction with the scaffold fibres. In Fig. 4(a), this was especially apparent where stromal actin filaments were wrapped around the scaffold fibres (circled), but was also true of epithelial cells (Fig. 4(b) circled). The fluorescence of the scaffold fibres also confirmed that cells were attached to multiple fibres. Some degree of alignment of the actin filaments with the scaffold fibres was also apparent, and this was particularly evident for the stromal cells (Fig. 4(a-b)).

Cell proliferation on PGA electrospun scaffolds seeded with either stromal cells alone or co-cultured with epithelial cells, seeded 24 h after stromal cell-seeding, was assessed by MTT. As the co-culture contained a mixture of cell types, and the standard curve for MTT optical density (OD) against cell number is specific to cell type [29], the number of cells growing in the co-culture construct could not be calculated, and are reported as OD (Fig. 4(c)). Although scaffolds were maintained for 14 days, the scaffolds on day 14 were

too fragile for an accurate assessment of cell proliferation; thus, only days 1-10 are shown (Fig. 4(c)). The MTT OD of scaffolds seeded with either stromal cells alone, or co-cultured with epithelial cells, increased over the 10 days of culture ($P < 0.05$, Fig. 4(c)). Despite a trend in higher OD observed on the co-culture scaffolds, there was not a significant effect of culture type, or a time × culture interaction (Fig. 4(c)). To confirm the ability of the scaffold to support epithelial cells, monoculture scaffolds seeded with epithelial cells alone were cultured for 10 days before staining with haematoxylin and eosin. Epithelial cells were present upon the scaffold, but only cells growing on the upper surface of the scaffold had a typical cuboidal, epithelial morphology (Supplemental Figure 1). Epithelial cells deeper within the scaffold had a predominantly striated morphology (Supplemental Figure 1).

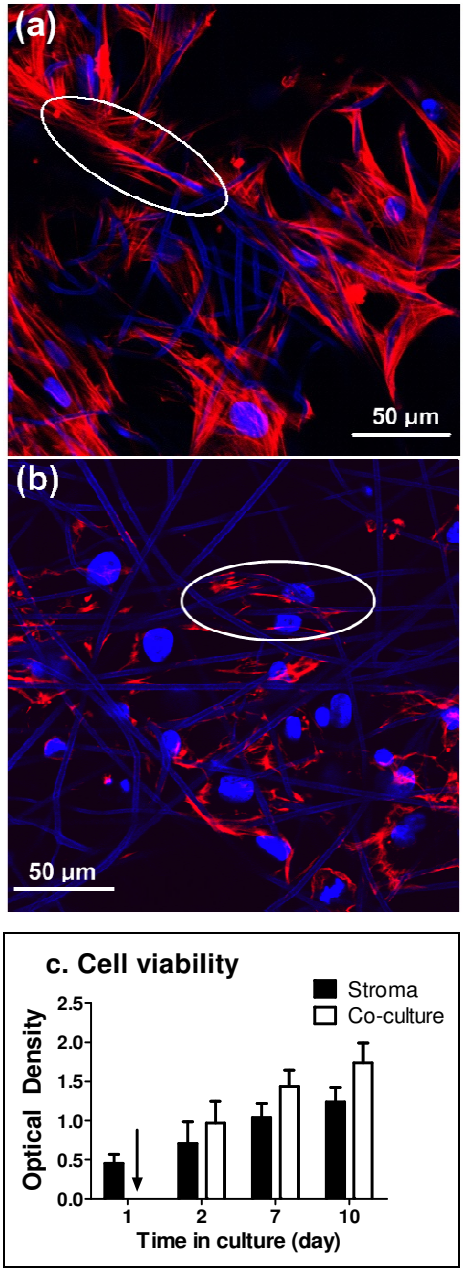


**Figure 4. Attachment of epithelial and stromal cells to electrospun PGA scaffolds. (a)** Stromal or **(b)** epithelial cells had filamentous actin staining (red). Actin filaments were wrapped around scaffold fibres (circles) on day 7 of scaffold culture. Hoechst 33258 was used as a nuclear stain, but also stained the scaffold fibres (blue). Scale bar = 50 µm. All images are representative of at least 4 fields of view from 3 independent experiments. **(c)** Cell viability, measured by MTT, of stromal cells seeded alone (■) or co-cultured with epithelial cells (□). Epithelial cells were seeded 24 h after stromal cell seeding, as indicated by the arrow. There was a positive correlation of cell viability over time, $P < 0.05$.

*Establishment of a stromal cell population on the PGA scaffold*

Having established that the electrospun PGA scaffold was biocompatible with both cell types, the dynamics of stromal cell growth upon the scaffold were then assessed. The cross sectional depth of the overall structure, from the apical surface to the basolateral surface of the construct, was measured using SEM images of the wax embedded sections of the scaffold (Fig. 5). Scaffolds were cultured for up to 14 days, but were too fragile to undergo the tissue processing for wax embedding, therefore were excluded from analysis for this time point.

There was a significant increase in the thickness of the stromal cell seeded scaffold constructs over time ($P<0.05$, Fig. 5(e)). On day 1, the stromal cell constructs had only a thin single cell layer that was difficult to measure, however by day 7 a cell mass was clearly evident (Fig. 5(d) and Fig. 6(a-c)), representing a significant increase in cellular growth upon the scaffold ($P<0.05$). The tissue thickness, whole construct thickness and cellular infiltration was similar between day 7 and day 10 of culture (Fig. 5 d-f)).

Upon examination of the construct cross sections, it was noted that the main cell mass, or tissue, formed on the upper region of the scaffold, with cells growing both within and on top of the scaffold (Fig. 5(a-c) and Fig. 6(b)). Therefore in addition to measuring tissue thickness (Fig. 5(d)), the depth that cells actually infiltrated into the scaffold was calculated (Fig. 5(f)). On day 1 of culture, stromal cells were present only on the top of the scaffold, with little evidence of cellular infiltration into the scaffold, but cells infiltrated deeper into the scaffold over time (Fig. 5(f) and Fig. 6(a&b)). By day 7, the upper half of the scaffold structure was predominantly infiltrated by tissue, although some individual cells were observed deeper in the scaffold (Fig. 5(f) and Fig. 6(b)).

The stromal cells seeded on PGA electrospun scaffolds also deposited fibronectin upon the scaffold (Fig. 6(d)). Fibronectin expression was particularly abundant at the periphery of the cell mass at the edge of the scaffold, appearing to anchor the edge of the cell mass to the scaffold, but

was also observed within the main stromal cell mass. Fibronectin expression was closely associated with scaffold fibres (Fig. 6(d)). The upper surface of the stromal seeded constructs had occasional areas with cuboidal-columnar epithelial-like cells growing on top of the stromal cell mass. These epithelial-like cells stained positive for cytokeratin, whereas the main cell mass was vimentin positive, cytokeratin negative.

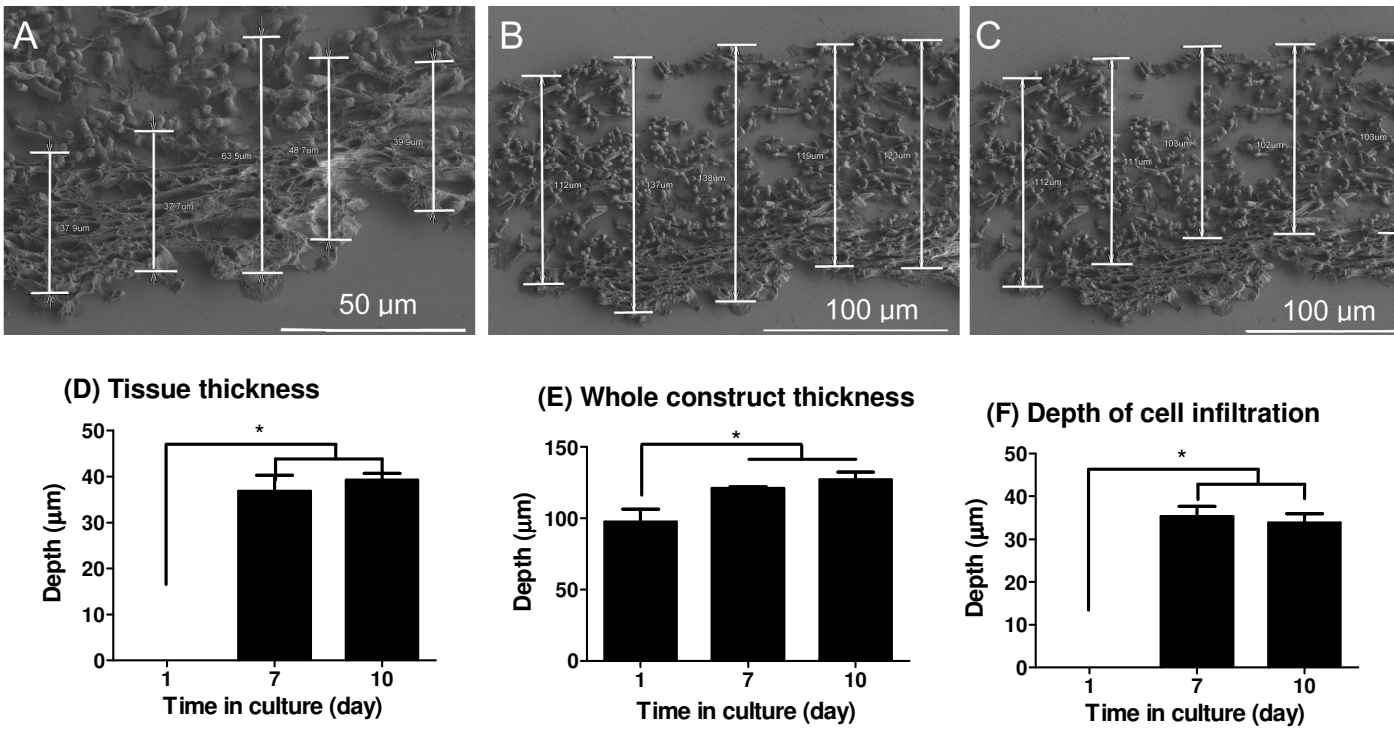


**Figure 5. Establishment of a stromal cell population on electrospun PGA scaffolds.** Stromal cells were seeded cultured alone as a stromal monoculture. **(a-c.)** Sample images depicting the measurements used to assess cellular g (**a**) tissue thickness, (**b**) whole scaffold construct thickness and (**c**) scaffold thickness, excluding the tissue growing on measurements for scaffold on days 1, 7, and 10 of culture for: . **(d)**; Tissue thickness, measuring cross sectional depth scaffold; **(e)** Scaffold construct thickness, measuring the full cross sectional depth of the scaffold construct **(f)** Depth scaffold, describes how deep into the scaffold the cells infiltrated. Data differ over time, *P < 0.05.

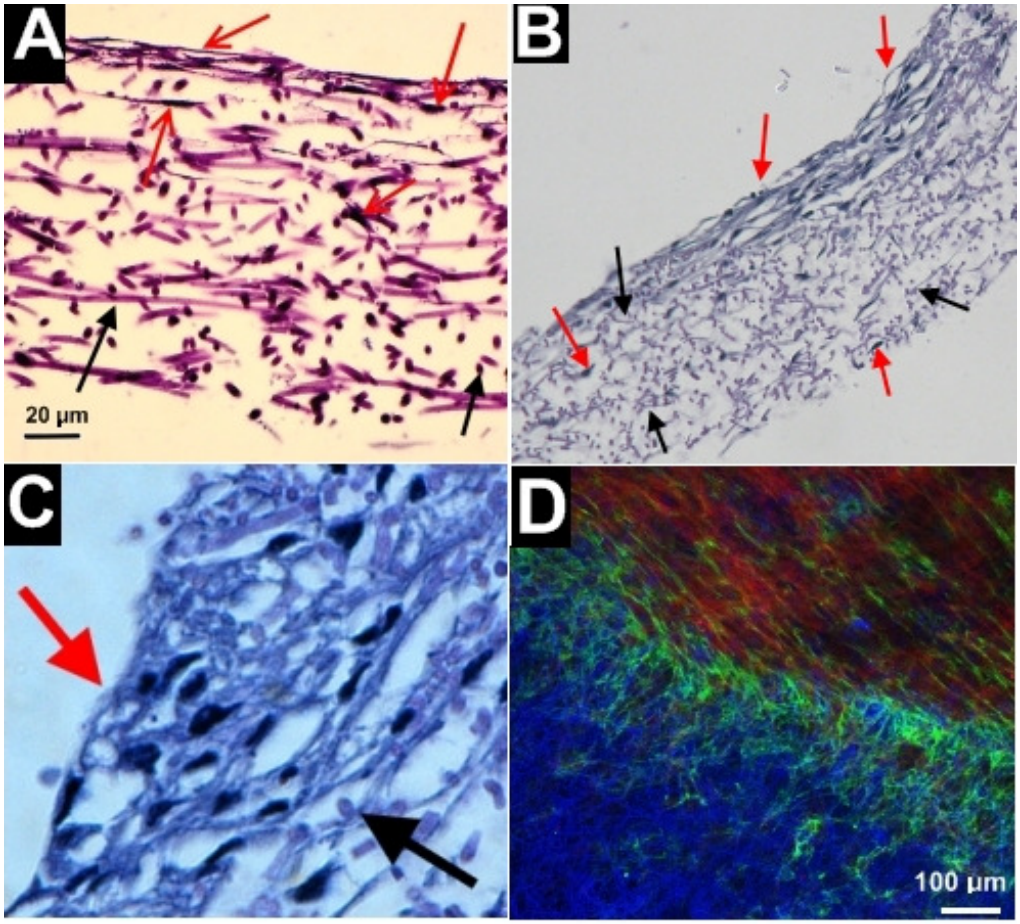


**Figure 6. Immunohistochemistry images of stromal seeded scaffolds. (a-c)** Haematoxylin and eosin staining of cross sectional sections of stromal cell-seeded PGA scaffolds on **(a)** day 7, or **(b and c)** day 10 of scaffold culture. Red arrows indicate cellular material, black arrows indicate scaffold fibres.. **(d)** Actin (red) and fibronectin (green) expression of the edge of a whole mount stromal cell-seeded PGA scaffold on day 10 of culture. Hoechst 33258 was used as a nuclear stain (blue). Scale bar = 100 µm. All images are of at least 4 fields of view from 3 independent experiments.

*Establish a co-culture of stromal and epithelial cells*

To develop a construct representative of endometrial tissue, two epithelial seeding protocols were compared, seeding stromal cells initially (day 0), and then seeding the epithelial cells on top of the stromal cells 24 h later on day 1 of scaffold culture (CCd1) or 7 days later (CCd7). Histological sections on day 7, 10 and 14 of scaffold culture are shown in Fig. 7. Epithelial cells with a cuboidal or columnar morphology were observed overlying the stromal cell mass on days 7 – 14 for the CCd1 constructs, and on days 10 and 14 for the CCd7 constructs (Fig. 7). However, on day 10 the stromal cell mass appeared larger, and the epithelial cell morphology was more uniform in the CCd1 constructs, compared to the CCd7 constructs (Fig. 7). On day 14 the scaffold constructs were very fragile and tended to fragment during handling, and the day 14 images in Fig. 7 represent fragments of the scaffold rather than an intact scaffold structure. Accordingly, all future work used CCd1 scaffolds from day 10 of culture.

To confirm the architectural arrangement of the two cell types in the co-culture scaffold, the CCd1 constructs were assessed for vimentin and cytokeratin expression (Fig. 8(a)). A single layer of cytokeratin positive, vimentin negative epithelial cells overlaid a stromal cell mass that was vimentin positive, cytokeratin negative (Fig. 8(a)). This represents a similar scenario to that seen in native endometrial tissue, although the epithelium of native tissue had a more uniform columnar epithelium than was observed upon the CCd1 construct (Fig. 8(a-b)). Furthermore, the epithelial cells on CCd1 construct expressed the tight junction-associated protein, zona occludens 1 (ZO-1), whereas scaffolds seeded with only stromal cells did not express ZO-1 (Fig. 8(c-d)). Apical expression of ZO-1 by epithelial cells was confirmed by z-stack imaging of the whole mount scaffolds (Supplemental Figure 2).

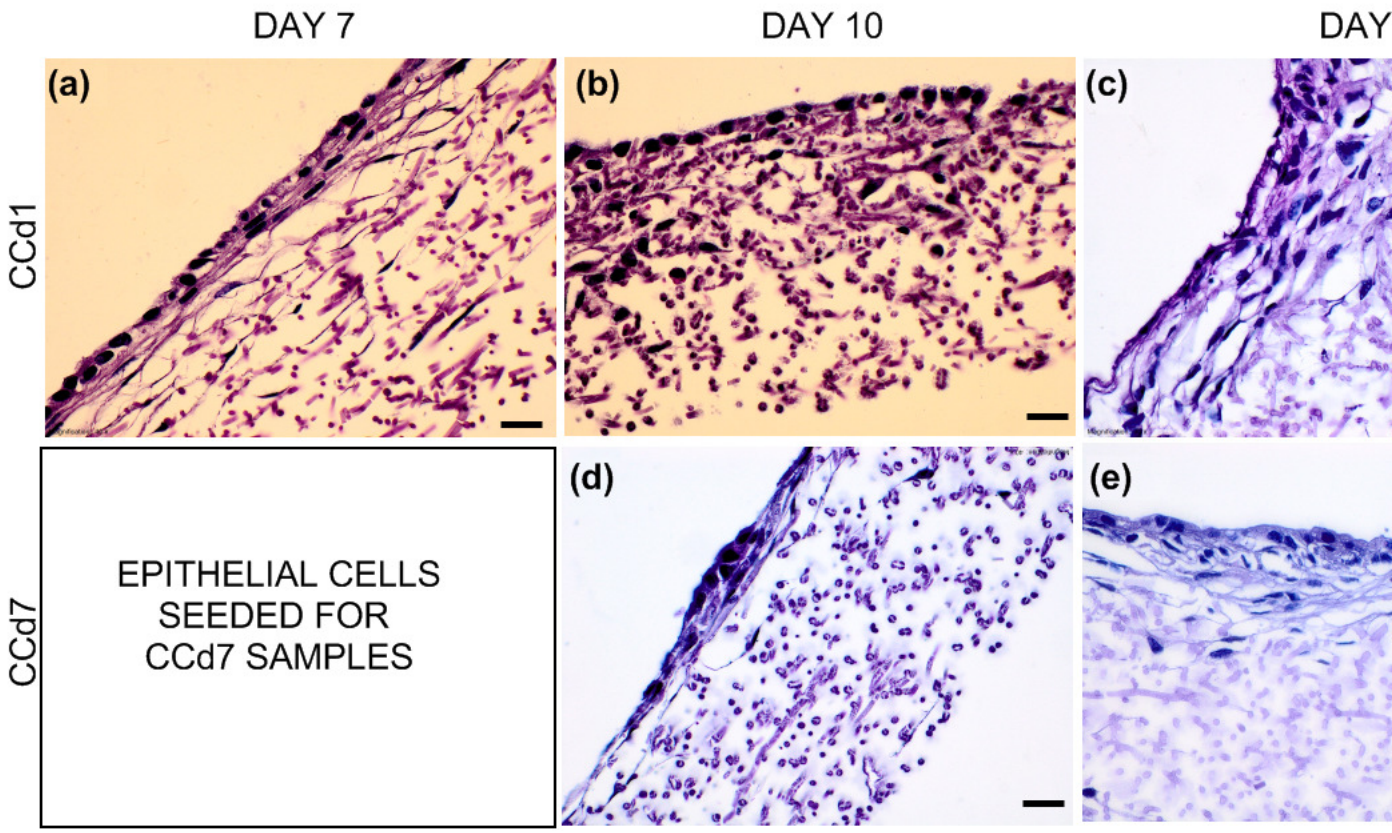


**Figure 7. Haematoxylin and eosin staining of co-cultured stromal and epithelial cells grown on electrospun**

seeded with stromal cells, and then epithelial cells were seeded either **(a-c)** 24 h later (day 1 of scaffold culture, CCd

CCd7. Cross sectional sections of the scaffolds from days 7, 10 and 14 of culture were stained using H&E to compa

morphology. Scale bar = 20 µm. All images are of at least 4 fields of view from 3 independent experiments.

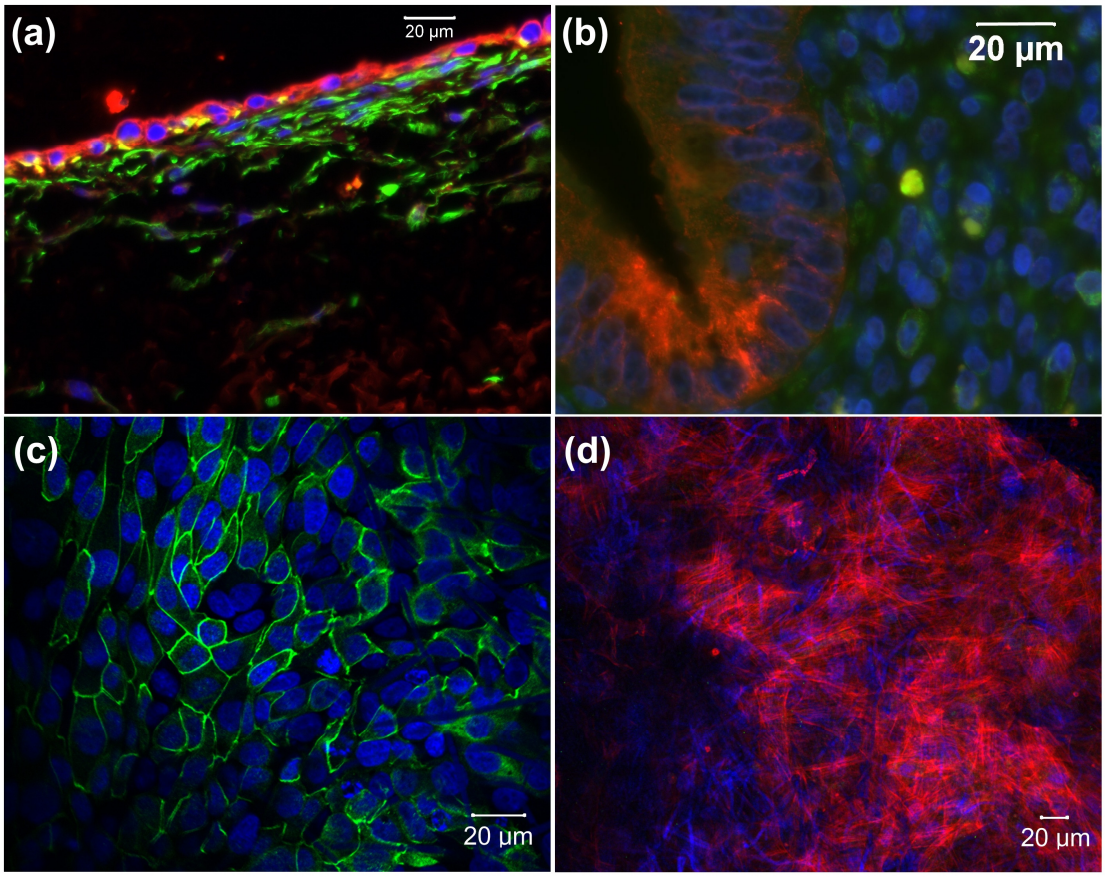


**Figure 8. Immunohistochemistry images of co-cultured stromal and epithelial cells seeded on electrospun PGA scaffolds on day 10 of culture. (a-b)** Cross sectional expression of cytokeratin (red) or vimentin (green) by endometrial cells on **(a)** a PGA scaffold (CCd1), or **(b)** within the bovine endometrium. **(c-d)** Cellular expression of actin (red) and ZO-1 (green) of whole mount scaffold constructs seeded with **(c)** stromal and epithelial co-culture (CCd1) or **(d)** stromal cells only. For all images, Hoechst 33258 was used as a nuclear stain and scale bars represent 20 µm. Images are representative of 4 fields of view from 3 independent experiments.

*Functionality of the co-culture endometrial construct*

To test the functionality of the endometrial constructs a co-culture of stromal and epithelial cells (CCd1) was grown for 10 days prior to treatment with OT+AA or LPS for 24 h. Both OT+AA and LPS stimulated an increase in PGE accumulation (Fig. 9). Accumulation of PGF was also significantly increased following OT+AA, but not LPS, treatment (Fig. 9).

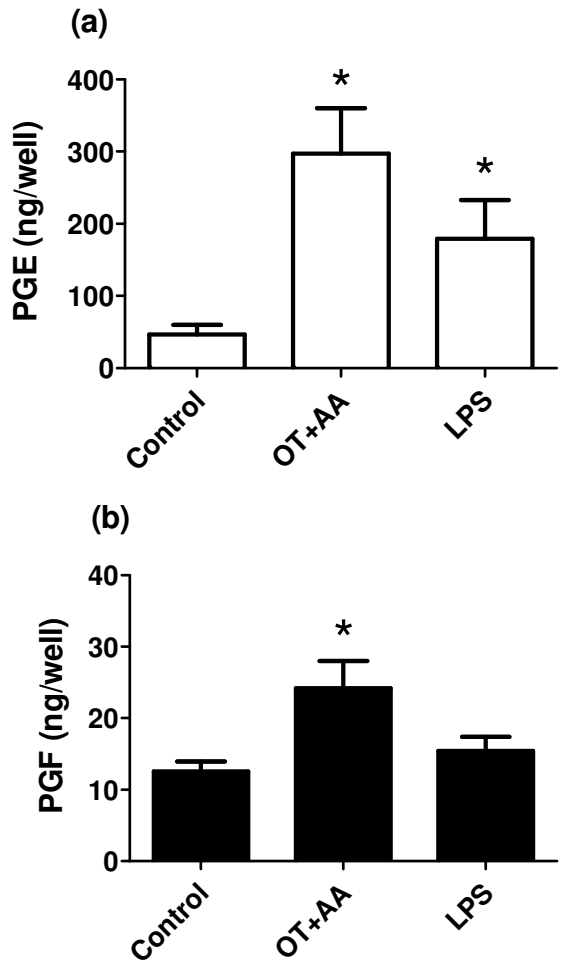


**Figure 9. Prostaglandin accumulation of endometrial cells seeded on electrospun scaffolds and treated with oxytocin plus arachidonic acid or LPS.** Accumulation of **(a)** PGE or **(b)** PGF following 24 h treatment of a co-culture scaffold (CCd1) with oxytocin plus arachidonic acid (OT+AA) or LPS. Supernatants were analysed using RIA, and data were analysed using ANOVA with Bonferroni post hoc. Prostaglandin accumulation differed between treated and control, *$P < 0.05$.

## 4. Discussion

In the present study, a PGA electrospun scaffold was selected to support the growth of endometrial constructs,. The PGA electrospun scaffold, had previously been used to support the growth of skin fibroblasts [25]. The PGA scaffold was compatible with both primary endometrial stromal and epithelial cells, based upon the attachment and proliferation of cells on the scaffold. The scaffold supported growth of multiple layers of stromal cells, overlaid by a single cell layer of epithelial cells, an architectural arrangement that is similar to *in vivo* endometrial tissue. Stromal cells deposited fibronectin upon the scaffold fibres, and actively wrapped actin filaments around the scaffold fibres. Epithelial cells had apical expression of the tight junction protein, ZO-1, and had a cuboidal to columnar morphology. Finally, the co-culture constructs cultured on PGA electrospun scaffolds were responsive to OT+AA and LPS treatment, validating the formation of a tractable 3D model of endometrium.

A significant advantage of the electrospun scaffold is that it represents a synthetic mimic of the ECM protein, collagen, providing an ideal framework to support tissue growth [7, 33]. Electrospun scaffolds have been widely used to support a variety of tissues, including human vascular tissue and skin but also bovine aorta endothelial cells [34-36], however as far as the authors are aware this is the first report of a bovine endometrial model grown on PGA electrospun fibres.

The PGA electrospun scaffold had randomly dispersed fibres with structural space for cell growth that was typical of a nonwoven electrospun material. This type of scaffold has a structure similar to collagen fibres *in vivo* [23]. The scaffold had interconnecting pores that varied in size, typical of electrospun scaffolds [23]. The PGA electrospun scaffold median pore diameter and maximum detected pore diameter were ~7.8 µm and ~11 µm respectively, as measured by capillary flow porometery. Capillary flow porometry measures the flow through pores and accounts for the smallest pores within the scaffold, and measured values are affected by fibre diameters, fibre and membrane mass thus estimated pore sizes may be more accurate than measurements taken using other techniques such as SEM, but may still be slightly lower than

the actual pores experienced by cells [37]. However the porosity of the scaffold used in the present study was sufficient for ingress of stromal and epithelial cells which have cell diameters of ~10 µm and ~15 µm respectively (measured from histological sections of endometrium, data not shown). This is part assisted by the flexible nature of electrospun fibres, which cells may be able to push aside as they migrate through the scaffold [33]. Migration of cells *in vivo* is maximal when the tissue fibre pore size is equal or slightly smaller than that of the cell [38]. *In vivo*, if tissue gaps are too large, then migration slows as a consequence of insufficient ECM-cell interaction. However if tissue gaps are too small then the ECM fibres provide a physical barrier to movement *in vivo* [38]. A similar effect of pore size/scaffold matrix thickness on cell migration is likely to occur *in vitro* when using scaffolds as a substitute for ECM.

A scaffold should support cellular attachment and growth, stimulate ECM deposition and have suitable porosity to support diffusion of gases, signalling molecules, nutrient and waste products to facilitate cell survival and differentiation [39]. In the preliminary experiments using the PGA electrospun scaffold to support the growth of both stromal and epithelial cells. Identification of a polymer that was compatible with both cell types was key, given the heterogenouos nature of the endometrium [40]. Confocal imaging of the cells demonstrated that the actin filaments of cells were wrapped around the scaffold fibres, indicating active attachment of the cells to the scaffold rather than cells being merely trapped within, but not interacting with the scaffold. Alignment of actin filaments along the scaffold fibres was also apparent. Cells are known to align with tissue structures *in vivo*, including blood vessels, muscle fibres and ECM fibres [38], and the observations of actin filament alignment along scaffold fibres in the present study may represent similar cell alignment behaviour to that as occurs *in vivo*.

Stromal cells seeded alone, or in co-culture with epithelial cells, proliferated within the scaffold over time. The ability of the scaffold to support epithelial cell growth was confirmed using histology and the epithelial cells growing on the upper surface of the scaffold assumed a typical morphology. Epithelial

cells growing in the deeper layers of the scaffold had predominantly an atypical epithelial morphology, which may represent some degree of differentiation due to a physical cue from the scaffold. *In vivo,* epithelial cells line the surface of mucosal tissue and display polarity, with cellular attachment via the lateral and basolateral membranes [41]. Epithelial morphology is directed by growth factors and hormones, and cues from the ECM [42]. The cues from the electrospun scaffold in the present study appeared to successfully support the growth of both cell types. Accordingly, subsequent work focussed initially on establishing stromal cells within the scaffold, upon which an epithelial cell suspension could be seeded.

In the scaffold, the main stromal cell mass was in the upper region of the scaffold, and grew both into and on top of the scaffold, giving rise to an increased thickness of the whole construct. The growth of stromal cells into the scaffold indicates that the porosity of the PGA scaffold was suited to cell migration and stromal cells were also observed within the deeper regions of the scaffold. A human endometrial 3D model observed spontaneous gland formation by epithelial cells within the stromal cell 3D constructs, possibly from contaminating epithelial cells within the stromal cell population, or from uterine stem cells that differentiated into epithelial cells during culture [10]. However, endometrial glands were not observed in the present study and further work on stem cells may be of interest for future models.

The stromal cells also deposited the ECM protein, fibronectin, with particularly strong expression at the edge of the cell mass (at the edge of the scaffold). Native ECM contains a diverse range of proteins, but fibronectin was selected for study as it is a ubiquitous component of the ECM, and has important roles in tissue function and wound healing [43]. Some parallels between wound healing and cellular population of an engineered scaffold may be perceived, as both require cellular infiltration, deposition of ECM and the formation of new tissue. In wound healing, cellular fibronectin is secreted in a compact form which must be unfolded and formed into a matrix, in a process that is cell mediated [43]. Different isoforms of fibronectin are associated with cell proliferation, attachment, migration and tissue organisation, and also promote

deposition of other ECM components [43]. In the present study, fibronectin deposition was clearly evident along the scaffold fibres, but also, to a lesser extent between cells in the main cell mass; indicating that the cells were depositing native ECM on the scaffold construct. The stimulation of native ECM deposition by cells on a scaffold fulfils another requirement of a scaffold structure [39].

Having established a stromal cell population on the scaffold, the timing of epithelial cell seeding was examined. Seeding of epithelial cells onto the stromal-seeded scaffold was attempted 1 or 7 days after stromal cells seeding. Whilst both seeding protocols resulted in polarised epithelial cells overlying multiple layers of stromal cells, the histology of CCd1 constructs on day 10 was more representative of native endometrial tissue than the CCd7 constructs, with more stromal cells within the scaffold, and the complete epithelialisation. The earlier seeding of epithelial cells may have had a beneficial effect on the proliferation of stromal cells. Co-culture of human endometrial stromal and epithelial cells increased epithelial proliferation, and was dependent on the release of stromal IGF-1 [44, 45]. However, co-culture of bovine endometrial stromal and epithelial cells, in which the two cell types were not in direct contact, did not alter the proliferation of either cell type [29]. Co-culture scaffolds had further improvements in cell morphology, regardless of the timing of epithelial seeding; but were incredibly delicate between days 12-14 of culture, making them very difficult to handle. Other studies have also reported the rapid degradation of PGA nanofibers which can render the scaffold construct fragile [16]. The electrospun PGA scaffold utilised here has been successfully used to culture skin fibroblasts [25]. Other studies report culturing electrospun scaffolds for ~10 days [23]. Therefore, in the present study subsequent work seeded epithelial cells 24 hours after stromal cell-seeding, and scaffold constructs were cultured for 11 days. This was sufficient to provide a multiple layer-stromal cell mass, overlaid by epithelium suitable for *in vitro* testing.

The CCd1 constructs had not only appropriate expression of cytokeratin and vimentin of native endometrium, but also apical expression of ZO-1 by

epithelial cells. The apical expression of ZO-1 confirms the polarisation of epithelial cells growing on the scaffold. Further work to enhance the establishment of endometrial cells may be beneficial for this model, however the construct still represents a closer mimic of endometrial tissue that can be achieved using 2D culture. Furthermore, the functionality of the endometrial constructs was tested by exposing the scaffolds to OT+AA or LPS on day 10 of culture for 24 h. Both treatments stimulated PGE accumulation, but only OT+AA stimulated increased accumulation of PGF as expected, based upon previous studies using 2D monocultures, or co-cultures of epithelial and stromal cells on a transwell insert, [27, 29, 46]. In contrast, explants produce both PGE and PGF in response to either OT+AA or LPS treatment [26, 47]. Appropriate PGE and PGF responsiveness of endometrial cells to OT+AA and LPS demonstrates that the constructs are functional.

The endometrial construct described in the present report contains only stromal and epithelial cells, however native endometrium also contains endothelial and immune cells. Although a reductionist approach, using the main two cell types to establish an endometrial model is useful, the incorporation of other relevant cell types into the scaffold model could be considered for future studies, as could the development of a model that contains endometrial glands.

## 5. Conclusion

In conclusion, a straightforward model is presented here to culture multiple layers of stromal cells growing in 3D on a PGA electrospun scaffold, overlaid by a polarised epithelium. The overall arrangement was similar to native endometrium, and the endometrial constructs were responsive to OT+AA and LPS after 10 days of culture. Whilst further study could improve this model, the constructs provide an enhanced culture of a defined cell population that better represents *in vivo* tissue. The availability of a sophisticated 3D model of endometrium will be advantageous for the study of disease and the development of therapies.

**6. Acknowledgements**

The authors would like to thank Dr J. Bromfield for his assistance and Zoetis (formerly Pfizer Animal Health) for funding support. S. MacKintosh was kindly supported by a BBSRC CASE doctoral training grant (grant: BB/D526761/1). The authors confirm that there are no known conflicts of interest associated with this publication.

## 7. References


[1] Hutmacher DW. Scaffold design and fabrication technologies for engineering tissues--state of the art and future perspectives. J Biomat Sci - Polym E. 2001;12(1):107-24.

[2] Brown RA, Phillips JB. Cell responses to biomimetic protein scaffolds used in tissue repair and engineering. Int Rev Cytol. 2007;262:75-150.

[3] Lee JJ, Lee SG, Park JC, Yang YI, Kim JK. Investigation on biodegradable PLGA scaffold with various pore size structures for skin tissue engineering. Curr Appl Phys. 2007;7(S1):37 - 40.

[4] Li WJ, Tuli R, Okafor C, Derfoul A, Danielson KG, Hall DJ, et al. A three-dimensional nanofibrous scaffold for cartilage tissue engineering using human mesenchymal stem cells. Biomaterials. 2005;26(6):599-609.

[5] Seol YJ, Kang TY, Cho DW. Solid freeform fabrication technology applied to tissue engineering with various biomaterials. Soft Matter. 2012;8(6):1730-5.

[6] Huh Y, Kim YY, Ku SY. Perspective of Bioartificial Uterus as Gynecological Regenerative Medicine. Tissue Eng Regen Med. 2012;9(5):233-9.

[7] Griffith LG, Swartz MA. Capturing complex 3D tissue physiology in vitro. Nat Rev Mol Cell Biol. 2006;7(3):211-24.

[8] Kim DH, Lipke EA, Kim P, Cheong R, Thompson S, Delannoy M, et al. Nanoscale cues regulate the structure and function of macroscopic cardiac tissue constructs. Proc Natl Acad Sci USA. 2009;107(2):565-70.

[9] Hjelm BE, Berta AN, Nickerson CA, Arntzen CJ, Herbst-Kralovetz MM. Development and characterization of a three-dimensional organotypic human vaginal epithelial cell model. Biol Reprod. 2010;82(3):617-27.

[10] Wang H, Pilla F, Anderson S, Martinez-Escribano S, Herrer I, Moreno-Moya JM, et al. A novel model of human implantation: 3D endometrium-like culture system to study attachment of human trophoblast (Jar) cell spheroids. Mol Hum Reprod. 2012;18(1):33-43.

[11] Schutte SC, Taylor RN. A tissue-engineered human endometrial stroma that responds to cues for secretory differentiation, decidualization, and menstruation. Fert Steril. 2012;97(4):997-1003.

[12] Yamauchi N, Yamada O, Takahashi T, Imai K, Sato T, Ito A, et al. A three-dimensional cell culture model for bovine endometrium: regeneration of a multicellular spheroid using ascorbate. Placenta. 2003;24(2-3):258-69.

[13] Saw SH, Wang K, Yong T, Ramakrishna S. Polymer Nanofibers in Tissue Engineering. In: Kumar CSSR, editor. Tissue, Cell, and Organ Engineering. 9 ed. Weinheim: Wiley-VCH Verlag GmBH & Co.; 2006. p. 66 - 134.

[14] Drewa T, Galazka P, Prokurat A, Wolski Z, Sir J, Wysocka K, et al. Abdominal wall repair using a biodegradable scaffold seeded with cells. J Pediatr Surg. 2005;40(2):317-21.

[15] Fu Q, Deng C-L, Zhao R-Y, Wang Y, Cao Y. The effect of mechanical extension stimulation combined with epithelial cell sorting on outcomes of implanted tissue-engineered muscular urethras. Biomaterials. 2014;35(1):105-12.

[16] Boomer L, Liu Y, Mahler N, Johnson J, Zak K, Nelson T, et al. Scaffolding for challenging environments: Materials selection for tissue engineered intestine. Journal of Biomedical Materials Research Part A. 2014;102(11):3795-802.

[17] Albers LL, Borders N. Minimizing genital tract trauma and related pain following spontaneous vaginal birth. J Midwifery Wom Heal. 2007;52(3):246-53.

[18] Javed F, Al-Askar M, Almas K, Romanos GE, Al-Hezaimi K. Tissue reactions to various suture materials used in oral surgical interventions. ISRN Dentistry. 2012;2012:762095.
[19] Cheung H, Lau K, Lu T, Hui D. A critical review on polymer-based bio-engineered materials for scaffold development. Composites: Part B. 2007;38:297-300.
[20] Nair LS, Bhattacharyya S, Laurencin CT. Nanotechnology and Tissue Engineering: The Scaffold Based Approach. In: Kumar CSSR, editor. Tissue, Cell and Organ Engineering. 1st ed. Weinheim: Wiley-VCH GmbH & Co.; 2006.
[21] Murugan R, Ramakrishna S. Nanophase Biomaterials for Tissue Engineering. In: Kumar C, editor. Tissue, Cell and Organ Engineering. 1st ed. Weinheim: Wiley-VCH; 2006. p. 216-56.
[22] Bonfield W. Designing porous scaffolds for tissue engineering. Philos T Roy Soc A. 2006;364:227-32.
[23] Li WJ, Laurencin CT, Caterson EJ, Tuan RS, Ko FK. Electrospun nanofibrous structure: a novel scaffold for tissue engineering. J Biomed Mater Res. 2002;60(4):613-21.
[24] Lee J, Jang J, Oh H, Jeong YH, Cho D-W. Fabrication of a three-dimensional nanofibrous scaffold with lattice pores using direct-write electrospinning. Materials Letters. 2013;93(0):397-400.
[25] Fry N, Dagger A, Morsley D, Lecomte H, Trayhearn R, Howard M, et al., inventors; Scaffold. United States of America patent US 8,338,402. 2012.
[26] Herath S, Fischer DP, Werling D, Williams EJ, Lilly ST, Dobson H, et al. Expression and function of Toll-like receptor 4 in the endometrial cells of the uterus. Endocrinology. 2006;147(1):562-70.
[27] Herath S, Lilly ST, Fischer DP, Williams EJ, Dobson H, Bryant CE, et al. Bacterial lipopolysaccharide induces an endocrine switch from prostaglandin F2alpha to prostaglandin E2 in bovine endometrium. Endocrinology. 2009;150(4):1912-20.
[28] Ireland JJ, Murphee RL, Coulson PB. Accuracy of predicting stages of bovine estrous cycle by gross appearance of the corpus luteum. J Dairy Sci. 1980;63(1):155-60.
[29] MacKintosh SB, Schuberth HJ, Healy LL, Sheldon IM. Polarised bovine endometrial epithelial cells vectorially secrete prostaglandins and chemotactic factors under physiological and pathological conditions. Reproduction. 2013;145(1):57-72.
[30] Fortier MA, Guilbault LA, Grasso F. Specific properties of epithelial and stromal cells from the endometrium of cows. J Reprod Fertil. 1988;83(1):239-48.
[31] Cheng Z, Robinson RS, Pushpakumara PG, Mansbridge RJ, Wathes DC. Effect of dietary polyunsaturated fatty acids on uterine prostaglandin synthesis in the cow. J Endocrinol. 2001;171(3):463-73.
[32] Poyser NL. Effects of various factors on prostaglandin synthesis by the guinea-pig uterus. J Reprod Fertil. 1987;81(1):269-76.
[33] Pham QP, Sharma U, Mikos AG. Electrospinning of polymeric nanofibers for tissue engineering applications: a review. Tissue Eng. 2006;12(5):1197-211.
[34] Zhu Y, Cao Y, Pan J, Liu Y. Macro-alignment of electrospun fibers for vascular tissue engineering. J Biomed Mater Res B. 2010;92(2):508-16.
[35] Min BM, Lee G, Kim SH, Nam YS, Lee TS, Park WH. Electrospinning of silk fibroin nanofibers and its effect on the adhesion and spreading of normal human keratinocytes and fibroblasts in vitro. Biomaterials. 2004;25(7-8):1289-97.
[36] Cheng Q, Lee BL, Komvopoulos K, Yan Z, Li S. Plasma surface chemical treatment of electrospun poly(L-lactide) microfibrous scaffolds for enhanced cell adhesion, growth, and infiltration. Tissue Eng Pt A. 2013;19(9-10):1188-98.

[37] Li D, Frey MW, Joo YL. Characterization of nanofibrous membranes with capillary flow porometry. J Membrane Sci. 2006;286(1-2):104-14.
[38] Friedl P, Wolf K. Plasticity of cell migration: a multiscale tuning model. J Cell Biol. 2009;188(1):11-9.
[39] Dhandayuthapani B, Yoshida Y, Maekawa T, Kumar DS. Polymeric Scaffolds in Tissue Engineering Application: A Review. Int J Polym Sci. 2011;2011:19.
[40] Cobb SP, Watson ED. Immunohistochemical study of immune cells in the bovine endometrium at different stages of the oestrous cycle. Res Vet Sci. 1995;59(3):238-41.
[41] Eaton S, Simons K. Apical, basal, and lateral cues for epithelial polarization. Cell. 1995;82(1):5-8.
[42] Streuli CH, Bailey N, Bissell MJ. Control of mammary epithelial differentiation: basement membrane induces tissue-specific gene expression in the absence of cell-cell interaction and morphological polarity. J Cell Biol. 1991;115(5):1383-95.
[43] To WS, Midwood KS. Plasma and cellular fibronectin: distinct and independent functions during tissue repair. Fibrogenesis Tissue Repair. 2011;4:21.
[44] Cooke PS, Buchanan DL, Young P, Setiawan T, Brody J, Korach KS, et al. Stromal estrogen receptors mediate mitogenic effects of estradiol on uterine epithelium. Proc Natl Acad Sci USA. 1997;94(12):6535-40.
[45] Pierro E, Minici F, Alesiani O, Miceli F, Proto C, Screpanti I, et al. Stromal-epithelial interactions modulate estrogen responsiveness in normal human endometrium. Biol Reprod. 2001;64(3):831-8.
[46] Asselin E, Goff AK, Bergeron H, Fortier MA. Influence of sex steroids on the production of prostaglandins F2 alpha and E2 and response to oxytocin in cultured epithelial and stromal cells of the bovine endometrium. Biol Reprod. 1996;54(2):371-9.
[47] Miller AN, Williams EJ, Sibley K, Herath S, Lane EA, Fishwick J, et al. The effects of Arcanobacterium pyogenes on endometrial function in vitro, and on uterine and ovarian function in vivo. Theriogenology. 2007;68(7):972-80.